

# ELECTROMAGNETIC STUDIES OF THE LITHOSPHERE AND ASTHENOSPHERE

GRAHAM HEINSON

*School of Earth Sciences, Flinders University, GPO Box 2100, Adelaide SA 5001, Australia*

(Received: 25 May, 1999)

**Abstract.** In geodynamic models of the Earth's interior, the lithosphere and asthenosphere are defined in terms of their rheology. Lithosphere has high viscosity, and can be divided into an elastic region at temperatures below 350 °C and an anelastic region above 650 °C. Beneath the lithosphere lies the ductile asthenosphere, with one- to two-orders of magnitude lower viscosity. Asthenosphere represents the location in the mantle where the melting point (solidus) is most closely approached, and sometimes intersected. Seismic, gravity and isostatic observations provide constraints on lithosphere-asthenosphere structure in terms of shear-rigidity, density and viscosity, which are all rheological properties. In particular, seismic shear- and surface-wave analyses produce estimates of a low-velocity zone (LVZ) asthenosphere at depths comparable to the predicted rheological transitions. Heat flow measurements on the ocean floor also provide a measure of the thermal structure of the lithosphere.

Electromagnetic (EM) observations provide complementary information on lithosphere-asthenosphere structure in terms of electrical conductivity. Laboratory studies of mantle minerals show that EM observations are very sensitive to the presence of melt or volatiles. A high conductivity zone (HCZ) in the upper mantle therefore represents an electrical asthenosphere (containing melt and/or volatile) that may be distinct from a rheological asthenosphere and the LVZ. Additionally, the vector propagation of EM fields in the Earth provides information on anisotropic conduction in the lithosphere and asthenosphere. In the last decade, numerous EM studies have focussed on the delineation of an HCZ in the upper mantle, and the determination of melt/volatile fractions and the dynamics of the lithosphere-asthenosphere. Such HCZs have been imaged under a variety of tectonic zones, including mid-ocean ridges and continental rifts, but Archaean shields show little evidence of an HCZ, implying that the geotherm is always below the mantle solidus. Anisotropy in the conductivity of oceanic and continental lithosphere has also been detected, but it is not clear if the HCZ is also anisotropic. Although much progress has been made, these results have raised new and interesting questions of asthenosphere melt/volatiles porosity and permeability, and lithosphere-upper mantle heterogeneity. It is likely that in the next decade EM will continue to make a significant contribution to our understanding of plate tectonic processes.

**Keywords:** lithosphere, asthenosphere, electromagnetism, magnetotellurics, electrical conductivity

## 1. Introduction

Unlike crustal studies, geophysical properties of the upper mantle must be inferred from surface or satellite measurements. Mantle xenoliths provide geochemical information on mantle petrology, but it is difficult to determine physical parameters from such samples that can be up-scaled to mantle properties. As a consequence,



*Surveys in Geophysics* **20**: 229–255, 1999.

© 1999 Kluwer Academic Publishers. Printed in the Netherlands.

and given the inherent non-uniqueness of interpretation, there are limited constraints on models generated by any single geophysical technique. Laboratory measurements and computational studies may reduce the uncertainty, but more often than not also lead to fresh paradoxes. In this review, the main question to be addressed is to what extent can EM measurements delineate the properties and boundary between lithosphere and asthenosphere in terms of electrical conductivity? In other words, what, if any, significant differences can be determined in terms of variations in conductivity, either with depth or laterally through the upper mantle?

The corollary to such a question is can we infer other physical properties from conductivity and relate these to the geology of the lithosphere and asthenosphere? Parkinson (1983) asserts that

delineation of underground electrical conductivity is little more than an elegant exercise unless the conductivity can be related to other physical variables,

However, an opposing view is put forward by Tozer (1979)

when the essential scientific aim in interpreting and relating observable quantities has been achieved by the assignment of a material property, what further scientific purpose, if any, is being served by efforts to reinterpret it as the value of a function depending on an ill-defined number of unobservable quantities existing at the same point?

While we may have some sympathy with Tozer's view, there are many reasons to undertake such a procedure. For example, it is of great value to distinguish melt fractions from solid rock and to place bounds on the porosity of a zone of study. Such interpretation requires an understanding of the physics of electrical conduction in rocks and minerals, both in sub-solidus and molten form. Recent laboratory conductivity measurements of mantle minerals and the associated theoretical insights gained have closed the gap between field observation and interpretation (e.g., Constable and Duba, 1990; Karato, 1990; Constable, Shankland and Duba, 1992; Duba and Constable, 1993; Roberts and Tyburczy, 1999).

The review will be developed from three directions. Firstly, the geophysical state of the lithosphere-asthenosphere system (based on seismic, geochemical and geodynamic evidence) will be briefly examined. Secondly, recent laboratory measurements of electrical conductivity of mantle minerals under typical mantle temperatures and pressures will be discussed. Finally, using selected examples, evidence from a variety of EM experiments for variations in lithosphere-asthenosphere conductivity will be outlined. The latter section shows that significant progress in our understanding has been made over the last ten years. Some of the questions that are currently being addressed by mantle-scale EM studies include:

1. What can EM data tell us about the melt fraction in the asthenosphere, and its migration? In addition to the volume of melt, can we determine melt connec-

tion? In other words, to what accuracy can we determine bulk melt-porosity of the asthenosphere and its permeability?

2. What is the role of fluids (H<sub>2</sub>O and CO<sub>2</sub>) in the upper mantle? Can we distinguish enhanced conductivities due to either melt and/or fluids?
3. At plate margins and active tectonic zones (mid-ocean ridges, subduction zones and continental extensional, compressional and translation regimes), can we delineate the structure of the upper mantle?
4. What can we learn about anisotropy in the lithosphere and asthenosphere?
5. How heterogeneous is the lithosphere and asthenosphere in terms of its electrical conductivity, and what might we expect to detect? Can we relate inhomogeneous conductivity to variations in lithosphere-asthenosphere mineralogy, temperature or melt?
6. At passive continental margins, how does continental-ocean lithosphere-asthenosphere structure connect?

Electromagnetic studies over the last ten years have made significant progress towards points 1, 2 and 3. The issue of anisotropy and the heterogeneity of the lithosphere (points 4 and 5) are starting to be addressed, as the quality and volume of data are increased. Continental passive-margin studies (point 6) are relatively few, but will probably increase over the next five years.

This review mainly covers published material from 1992–1998, since Cohn Brown's review at the 11th EM Workshop in Wellington. It follows on from reviews given by Brown (1994) on regional conductivity anomalies of the crust and mantle; Tarits (1994) on global geodynamic processes; and Palshin (1996) on oceanic electromagnetic studies. Simpson (1999) gives a review of continental lower crustal processes.

## 2. Lithosphere–Asthenosphere Structure

The distinction between lithosphere and asthenosphere is primarily controlled by rheology. Figure 1 shows the generalised relationship between rigidity of the lithosphere-asthenosphere beneath oceans and continents (Molnar, 1988; Watts et al., 1980). Ductile flow at the base of the lithosphere (shown in Figure 1 at about 100 km) occurs due to thermally activated power-law creep and diffusion creep. Power-law creep takes place by the motion of dislocations on glide planes. The strain rate has an exponential dependence on temperature, and is found to be the most important creep mechanism at temperatures between about 600 and 1000 °C. This temperature range approximately corresponds to that of the lower lithosphere. At greater depths and at temperatures greater than 1000 °C, diffusion creep is dominant, due to thermally activated migration of crystal defects in the presence of a stress field. As indicated schematically in Figure 1 the transition between a rigid lithosphere and a viscous asthenosphere is gradational. The range of viscosity of

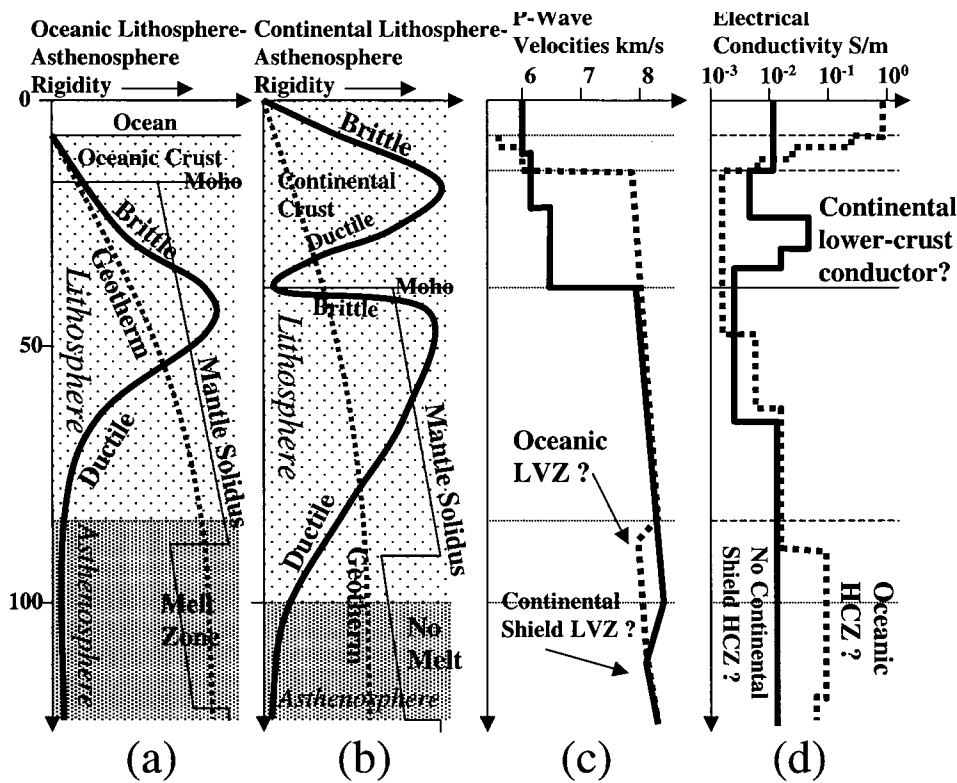


Figure 1. Schematic figures showing vertical profiles of rigidity (solid thick line), mantle geotherm (dashed line) and mantle solidus (thin solid line) in (a) oceanic upper mantle, and in (b) continental upper mantle. Note that the mantle solidus is reduced at asthenosphere depths due to the presence of volatiles (Ringwood, 1975); if the geotherm intersects the solidus then partial melting occurs. The lithosphere-asthenosphere transition is determined by the change from brittle to ductile rheology. Figure 1(c) shows typical P-wave velocities through a continental shield (solid thick line) and oceanic lithosphere (dashed line). A more pronounced LVZ occurs at shallower depths beneath the ocean basins. Figure 1(d) shows typical electrical conductivity structures below a continental shield (solid thick line) and oceanic lithosphere (dashed line). A HCZ is often found under oceanic lithosphere and in areas of continental extension. (Figures (a) and (b) adapted from Molnar (1988), Watts et al. (1980) and Parsons and Sclater (1977); Figure (c) adapted from Lay and Wallace, 1995).

the lithosphere is great, ranging from infinite (for a rigid media) to  $10^{21}$  Pa.s at the base, while the asthenosphere has a lower viscosity  $10^{19}$ – $10^{21}$  Pa.s.

The asthenosphere represents the location in the mantle where the melting point (solidus) is most closely approached. Temperatures below the asthenosphere are higher (from about 1300–1500 °C), but the upper mantle to the transition zone has an increased viscosity  $10^{21}$  Pa.s as the mantle solidus increases with depth faster than the upper mantle temperature. Asthenosphere therefore represents a mechanical boundary between more rigid regions above and below. In some places, asthenosphere must be partially molten, but this is not necessarily the case every-

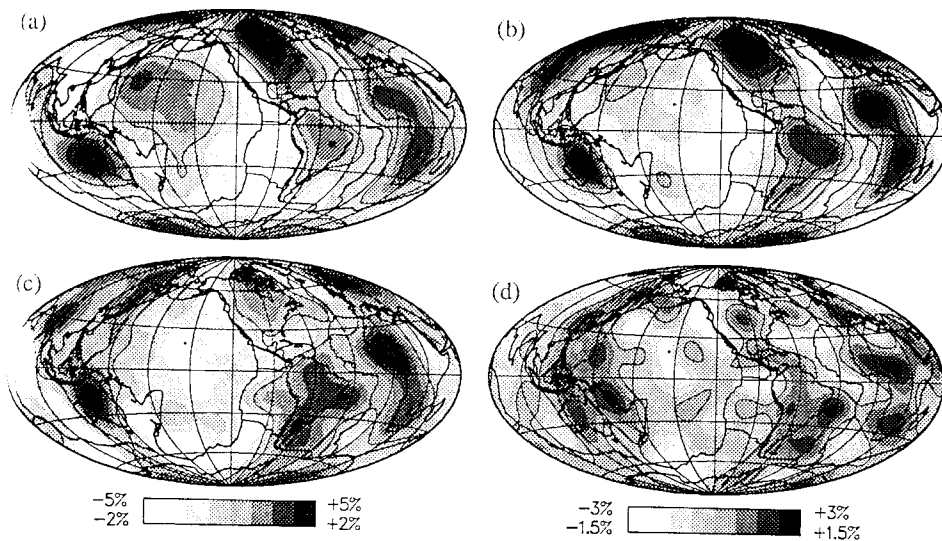


Figure 2. Global shear-wave velocity heterogeneity at 50, (b) 150, (c) 250 and (d) 350 km, from Love and Rayleigh wave dispersion observations, determined to spherical harmonic order 12 (Su et al., 1994). The fastest regions (black) are under the shield areas of Australia, Canada, Siberia; low velocity zones (LVZs) (white) are shown under the mid-ocean ridges to a depth of 150 km. The scale bars show velocity variations from the PREM model as a percentage; different scales apply for each model. (© by the American Geophysical Union).

where; the volume and lateral extent of melting in the asthenosphere is unknown. From geodynamical considerations of melt in porous media (McKenzie, 1989; Shankland and Waff, 1977), melt fractions must be small to be gravitationally stable. However, Faul (1997) has shown that melt fractions of up to 3% are possible if the permeability is sufficiently low.

Some of the best constraints on lithosphere-asthenosphere structure are provided by global seismic-wave analysis. Shear waves are slowed in the low-rigidity asthenosphere due to the reduced viscosity. An analysis of surface wave dispersion indicates the presence of a LVZ at depth that broadly corresponds with the rheological asthenosphere. The LVZ is shallowest beneath the mid-ocean ridges and is imaged at greater depths under older oceanic lithosphere. Beneath continental lithosphere, LVZs are sometimes detected in active tectonic regions, but are often absent below shield areas where the lithosphere is thickest. Tomographic reconstructions of anomalous shear-wave velocities at depths through the upper mantle are shown in Figure 2 (Su et al., 1994). Shear-wave velocities are determined on a spherical harmonic model to degree 12; differences from the PREM model are as much as 5%. Note that only continent sized features are resolved. Higher resolution studies (e.g., van der Hilst et al., 1997) show more detailed heterogeneity of 1998) scale-lengths of a few tens of kilometres. It seems plausible that mantle seismic heterogeneity exists at different scale-lengths worldwide.

To obtain velocity anomalies of 5%, an associated thermal anomaly of several hundred degrees is required, with slower velocities in hotter mantle (Lay and Wallace, 1995). The presence of partial melt will reduce the shear-wave rigidity-modulus further. Localised temperature perturbations are likely to be even larger than can be imaged by the limited spatial resolution of the tomographic model. Fluid dynamical calculations indicate that resulting density variations will drive solid-state convective motions of the upper mantle over long time-scales.

The models in Figure 2 show that the most seismically-heterogeneous region of the upper mantle is within the top 100 km. Low-velocity zones are centred over the mid-ocean ridges, particularly evident across the East Pacific Rise. With increasing depths, the LVZs broaden, and at a depth of 250 km they are quite diffuse. At greater depths, the LVZs can still be identified with the mid-ocean ridges, but hot spots such as Hawaii and Tahiti also show a broad-scale anomaly which is almost circular. Beneath continental shields (for example western Australia and northeastern Canada), shear-wave velocities are up to 5% faster than the PREM model, indicating a more rigid upper mantle to 400 km and implying the lack of a low-rigidity asthenosphere. An increase in rigidity suggests that the geotherm is significantly lower than in non-shield areas, and consequently that the continental lithosphere is much thicker and there is little or no partial melt in the asthenosphere.

The thickness of the oceanic lithosphere can be well determined from heat flow measurements and ocean depth (Parsons and Selater, 1977), and from seismic surface waves (Zhang and Lay, 1996). Both methods are in good agreement with the observed data, except for the oldest parts of the seafloor ( $>140$  Ma), suggesting a less pronounced thickening of the plate with age. Close to the ridges the lithosphere is probably less than 50 km thick, increasing in thickness to 100 km for the oldest parts of the seafloor (180 Ma). Oceanic asthenosphere thickness is more difficult to determine from seismic-wave analysis because the low velocities do not refract energy back to the surface. The tomographic inversions of Figure 2 and studies of the seismic attenuation factor  $Q$  (Lay and Wallace, 1995) suggest that shear-wave velocity heterogeneity can exist down to 350 km, while the compressional-waves heterogeneity is confined to the upper 250 km.

It is more difficult to determine continental lithosphere thicknesses from heat flow measurements due to the presence of radioactive isotopes within the continental crust. A measure of continental lithosphere thickness can be estimated from isostatic studies. For example, isostatic rebound of Fennoscandia following the disappearance of the ice sheet 10,000 yr. ago has been used to determine the density and rigidity of the upper mantle (e.g., Cathles, 1975), but estimates are non-unique and depend critically on asthenosphere viscosity. Gravity and seismic studies of continental lithosphere show considerable lateral variations in lithosphere elastic thickness. Beneath the Archaean shield areas lithosphere has been estimated to be greater than 150 km thick. In contrast, zones of lithosphere extension indicate asthenosphere as shallow as 40 km. For many continental regions, the presence of a LVZ is weakly defined, if at all, suggesting there is little or no melt present.

A property of the upper mantle that is still in a very early stage of being mapped is local- to regional-scale anisotropy. For oceanic lithosphere, seismic surface-wave analysis has proved to be useful, as a single wave travels through the lithosphere in the manner of a wave-guide (Tanimoto and Anderson, 1984; Ribe, 1989). Figure 3 shows the fast orientation of surface waves for a period of 200 s. Such anisotropy reflects the directions of plate motions and most probably indicates alignment of the [1 0 0] axis of olivine. Beneath the continental regions, anisotropy is less well determined, due to the much higher percentage of garnet-eclogites. Unlike olivine, garnet is almost isotropic, exhibiting only marginal variations in elastic properties with crystal orientation. However, anisotropy has been observed in continental lithosphere in a variety of tectonic regions, which may reflect crystal orientation from either current or palaeo-stress in the lithosphere-asthenosphere. The vertical and lateral extent of continental lithosphere anisotropy, and whether this extends to the asthenosphere, is largely unknown.

Chemically, the oceanic lithosphere is relatively simple beneath most of the ocean basins. As oceanic lithosphere is created at mid-ocean ridges, the geochemical signature imparted remains until the plate is subducted. Oceanic crust is remarkably uniform everywhere, in spite of the variable rates of accretion at the world's mid-ocean ridges. Lithosphere beneath the crust grades from a depleted harzburgite (about 80% olivine and 20% orthopyroxene) to lherzolite (about 60–70% olivine, 30% clinopyroxene and orthopyroxene, and minor amounts of garnet). The upper mantle source of the lherzolites are of peridotitic composition, sometimes referred to as pyrolite (Ringwood, 1975). There is no evidence that the lithosphere-asthenosphere boundary marks a phase change.

Continental lithosphere is very chemically heterogeneous. It has built up through accretionary processes at subduction zones and may contain magmas, entrapped sediments and bodies of eclogite derived from the melting of subducted basalt. Generation of secondary granitic magmas leads to differentiation of lower continental crust. Eclogites are high-pressure, low-temperature metamorphic rocks whose bulk composition closely resembles basalt (about equal amounts of aluminium pyroxene and garnet). The bulk of the continental lithosphere has a more peridotitic composition, comprising olivine and pyroxene phases.

Ringwood (1975) argues that volatile phases ( $\text{H}_2\text{O}$  and  $\text{CO}_2$ ) in the upper mantle are of the order of 0.1%. Above 75 km depth, water is held in amphiboles which is stable at temperatures below 1150 °C. Between 75–150 km, amphibole is no longer stable due to pressure-induced transformation, and water is liberated as a free phase that dramatically lowers the melt solidus causing the onset of melting. The free fluid-phase is highly partitioned into melt, as evident from mid-ocean ridge basalt analysis, which contain 0.2 to 0.5% water. Consequently, where melt has been extracted (at mid-ocean ridges, hot spots, subduction zones and in some extensional zones) the upper mantle will be dehydrated. Between 150–300 km, water is again stable in various hydroxylated silicates. Hirth and Kohlstedt (1996) give a full discussion on hydrous phases in the mantle.

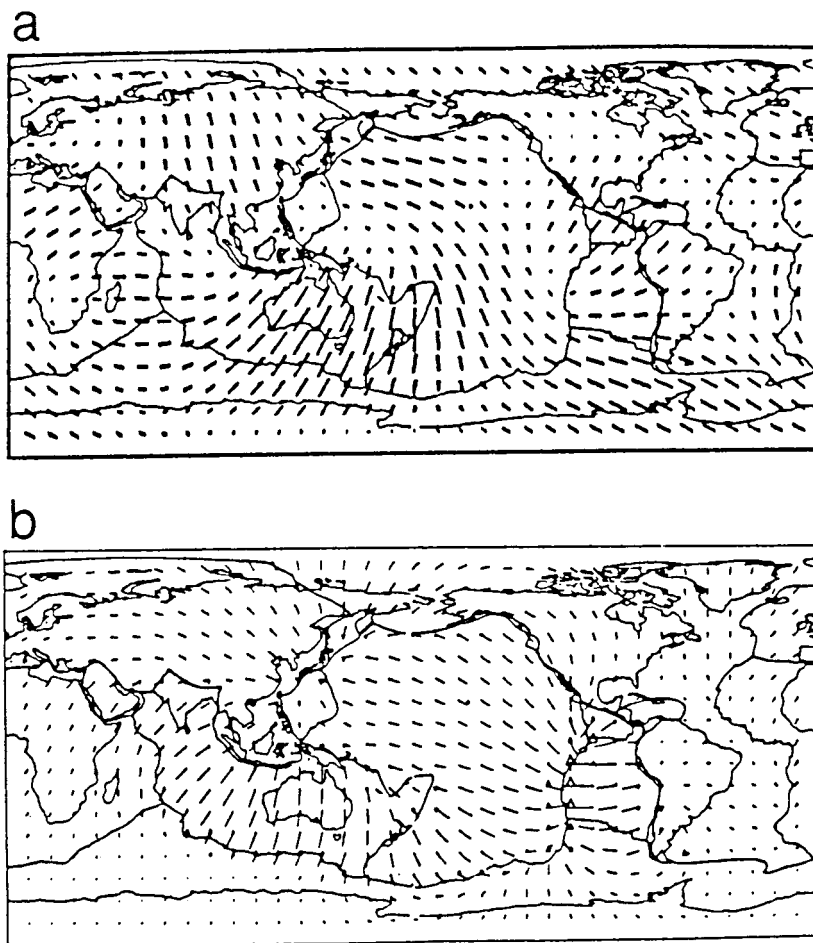


Figure 3. (a) Anisotropy in Rayleigh-wave phase velocities for a period of 200 s, which is most sensitive to structure between 150–300 km depth (Tanimoto and Anderson, 1984). The length of the lines is proportional to the extent of anisotropy, which is probably due to alignment of olivine. (b) Flow lines at a depth of 260 km for a kinematic plate tectonics model with a low viscosity channel in the upper mantle (from Hager and O'Connell, 1979). (Both figures © by the American Geophysical Union).

### 3. Laboratory Studies of Mantle Mineral Conductivities

In the last ten years, there have been major developments in laboratory studies of mantle mineral conductivities. Progress relevant to this review has been made in three main areas. Firstly, basic relationships between sub-solidus olivine conductivity and temperature have been firmly established (Shankland and Duba, 1990; Constable and Duba, 1990; Constable et al., 1992; Duba and Constable, 1993; Hirsch et al., 1993). Roberts and Tyburczy (1991, 1993, 1994) have also examined frequency- dependent electrical properties of mantle minerals.



One of the most useful empirical results to emerge from these studies is the 502 relationship between olivine conductivity and temperature is shown in Figure 4 (Constable et al., 1992). It is not obvious as to whether laboratory measurements on single crystals or composite over short periods of time (and at atmospheric pressure) can be up-scaled to represent the entire upper mantle. However, there is remarkably good agreement between laboratory measurements on different mantle and synthetic olivine samples and lherzolites, indicating good self-consistency. In Figure 4, a temperature of 1400–1500 °C is approximately that of the 400 km transition zone and the Moho may have a temperature of between 300–500 °C; the x-scale on Figure 4 can therefore be read as approximately a depth scale through the upper mantle. For typical mantle temperatures, the conductivity of olivine will be less than 0.004 S/m. Moreover, by assuming a temperature at the base of the lithosphere to be 1300 °C (Parsons and Sclater, 1977), the 502 model implies lithosphere conductivity of less than 0.001 S/m. Even with temperature perturbations of several hundred degrees (as inferred from seismic wave tomography) conductivity will vary by less than one order of magnitude. Such low conductivities are rarely encountered in long-period EM studies.

The second development has been in the understanding of melt in the mantle. Many long-period EM observations are interpreted with an HCZ of conductivity at least one order of magnitude greater than that predicted from 802, particularly at depths greater than 70 km (Heinson and Constable, 1992). In many instances, the presence of melt (Shankland and Waf, 1997) or volatiles (Tarits, 1986) were invoked to increase the conduction. However unreasonably large amounts of fluids were required (greater than 5%) which would not be gravitationally stable. The paradox promoted searches for alternative explanations, including the pervasive coast effect (Heinson and Constable, 1992) and the presence of mobile charged hydrogen ions (Karato, 1990).

Melt distributions analyses by Faul et al. (1994) and Faul (1997) show that most melt resides in low aspect-ratio, disk-shaped inclusions on two grain boundaries for melt percentages of 0.8–3%. The tubules interconnect, but have small cross-sectional areas compared with the inclusions, leading to a low permeability ( $k = 10^{17} \text{ m}^2$ ), and segregation velocities of less than  $1 \text{ mm yr}^{-1}$ . Roberts and Tyburczy (1999) detail an extensive study of melt conductivity based on experimental studies and using the MELTS programme of Ghioso and Sack (1995). Figure 5 shows measured conductivity versus melt volume fraction from this study with various models of melt conductivity. Roberts and Tyburczy's work shows that high conductivities of 0.1–0.001 S/m occur with about 5% melt fraction, and although the melt is connected it has low permeability ( $k = 10^{14} - 10^{18} \text{ m}^2$ ), and hence is stable.

Finally, exciting new studies of the conductivity of the  $\beta$ -spinel phase have indicated that there exists a one- to two-orders of magnitude jump in conductivity at the 400 km transition zone (Xu et al., 1998). With long-period EM measurements it is not possible to resolve the depth of such an increase, but it is clear that

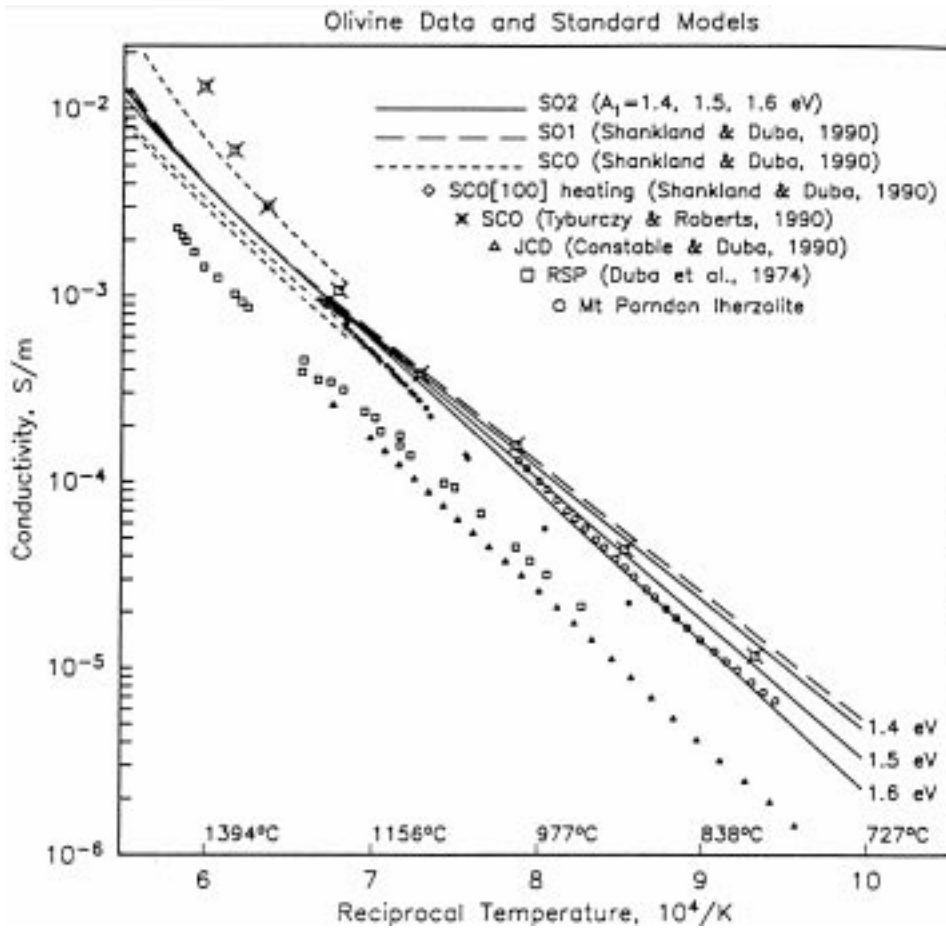


Figure 4. Conductivity versus temperature for various olivine samples, and model fits. Note in particular the 502 models (with different activation energies). Figure from Constable et al. (1992, © by the American Geophysical Union).

high conductivities of 1–0.1 S/m exist below 400 km. The existence of a rapid rise in conductivity below 400 km has profound implications for upper mantle EM studies. Given the resolution kernels of long-period EM observations, surface EM responses will necessarily average the conductivity jump over a broad range of depths, and as a consequence, smooth inversions of a jump in conductivity at 400 km will result in upper mantle conductivities that are too high.

#### 4. EM Studies of Oceanic Lithosphere and Asthenosphere

The EM methods used to probe the mantle to depths of a few hundred kilometres are primarily magnetotellurics (MT) and geomagnetic depth soundings (GDS). In

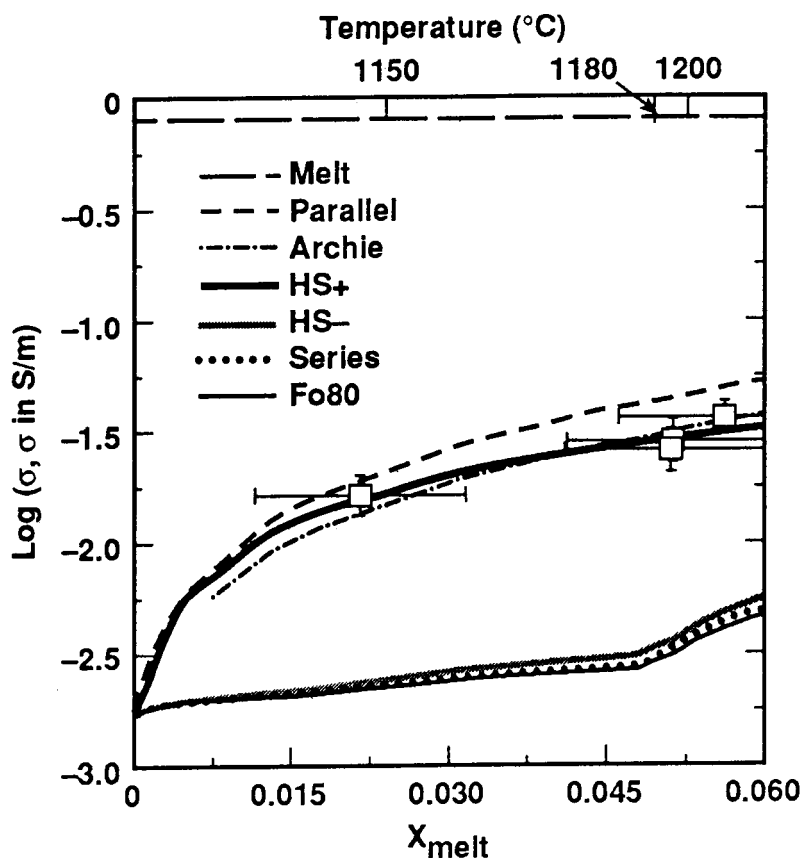


Figure 5. Log conductivity versus melt volume fraction ( $X_{\text{melt}}$ ) for various mixing models incorporating melt volume fraction as a function of temperature. Melt conductivity is constant at 0.8 S/m; crystalline conductivity is that of Fo80 (Hirsch et al., 1993), and is temperature dependent. Various theoretical models (e.g., Parallel, Archie etc.) of porosity-conductivity are shown as solid and dashed lines. The error bars show experimentally determined bulk conductivities, which fall approximately on the Hashin-Shtrickman upper bound, indicating parallel conduction through interconnected melt pathways. Figure taken from Roberts and Tyburzcy (1999, © by the American Geophysical Union).

some places, controlled source EM can also provide constraints on upper mantle processes. Resolution of structure in the upper mantle depends on the lateral sampling density and frequency bands used. Typically, vertical resolution is about 5–10% of depth, with comparable lateral resolution if the station spacing and skin depths are appropriate. In general, it is easier to resolve increases in conductivity, but it is not so easy to determine conductivity and thickness independently. In other words, a thin electrical asthenosphere may produce the same response as a thicker asthenosphere with lower conductivity.

Palshin (1996) and Brown (1994) give recent reviews of oceanic EM studies. Ocean floor EM experiments can be divided into two categories; those which use low-frequency (1–10 Hz) MT and GDS methods to probe the upper mantle struc-

ture, and controlled source EM studies for ocean crustal structure using higher frequencies (24–0.25 Hz). Magnetotelluric fields are small at high-frequencies due to attenuation through the seawater layer (Filloux, 1987), so most effort has been focused on the lithosphere-asthenosphere structure. Because there is a slight overlap in the MT and EM bandwidth, in some circumstances MT can be used for crustal exploration, and controlled source EM provides upper mantle constraints.

#### 4.1. MID-OCEAN RIDGES

Since Palshin's review, the most significant new marine MT experiment has been MELT (Mantle Electromagnetic and Tomographic Experiment) (Forsyth and Chave, 1994), combining MT and seismic tomography to investigate the structure of the East Pacific Rise. Two MT transects crossed the ridge along the most two-dimensional segment of the ridge, with a full spreading rate of 150–162 mm/yr. The objective of the experiment was to distinguish between two models of mantle upwelling and melt migration beneath a mid-ocean ridge. Initial results (Evans et al., 1999) show an asymmetry in conductivity between the western and eastern flanks of the ridge. To a depth of 100 km, the conductivity beneath the Nazca Plate is less than that beneath the Pacific Plate, suggesting high temperatures in the upper mantle. High temperatures would be consistent with the seafloor topography, which is slightly higher on the western side of the East Pacific Rise. Below 100 km, the conductivity is between 0.05 and 0.1 S/m, higher beneath the Nazca Plate.

The RAMESSES experiment in October 1993 (Sinha et al., 1997) took place across the slow-spreading Reykjanes Ridge (full rate of 40 mm/yr), which forms part of the Mid-Atlantic Ridge. One-dimensional interpretations of the along-axis MT data are shown in Figure 6. Sinha et al. (1997) interpreted these models in terms of a crustal magma chamber, sub-solidus lithosphere and asthenosphere below 50 km. Crustal and asthenosphere conductances were estimated to be approximately 800 S and 5000 S respectively, from which an asthenospheric melt porosity of 5% was calculated from Archie's Law. From observed MT anisotropy between TE and TM modes, there was little evidence for melt connection from the asthenosphere to the crustal magma chamber.

Heinson et al. (1996) and Constable et al. (1997) performed a similar small-scale MT experiment above Axial Seamount on the medium-spreading Juan de Fuca Ridge in the northeast Pacific Ocean. The seamount is part of the Cobb–Eikleberg chain, and currently intersects the ridge axis, so is not strictly representative of mid-ocean ridge processes. A one-dimensional interpretation is shown in Figure 6. Unlike other MT observations on the Juan de Fuca Plate and Ridge (Wannamaker et al., 1989; Heinson et al., 1993), the data showed little anisotropy, low apparent resistivities (10–20  $\Omega$ m at all frequencies) and nearly uniform phases ( $\sim 45^\circ$ ). The model in Figure 6 is more conductive than the Reykjanes Ridge, with slight increases over the crust (conductance 1200 S) and at depths 40–100 km. Heinson et al. (1996) suggested that the model indicated melt connection through

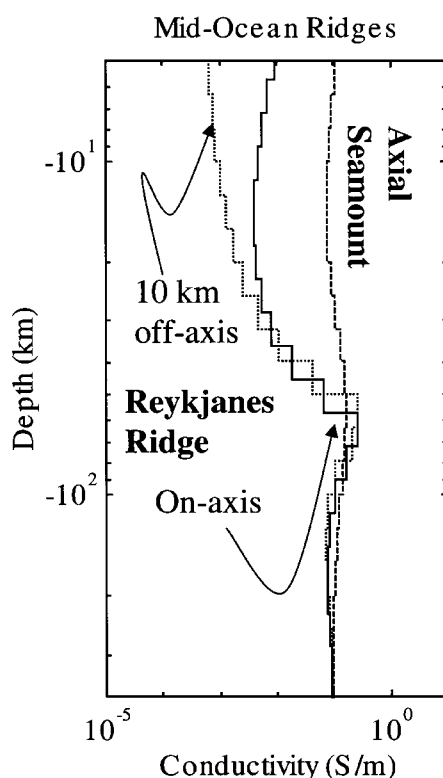


Figure 6. Mid-ocean ridge conductivity profiles, from 5 to 400 km below seafloor. Inversions of MT data collected at the Mid-Atlantic Ridge for sites on-axis (solid line) and 10 km off-axis (dotted line) (Sinha et al., 1997), and above Axial Seamount on the Juan de Fuca Ridge (dashed line) (Constable et al., 1997) are shown. An electrical asthenosphere from 50–100 km is evident, with conductivity 0.1 S/m. Inversions for sites directly above the ridge axis also show a high crustal conductivity.

the mantle from a primary source below 50 km to a magma chamber in the crust. Jegen and Edwards (1998) found a similar result across the Explorer Ridge north of Axial Seamount. Melt percentages of between 5–20 and 1–10% were determined for the crust and mantle respectively. The lateral extent of melting beneath the hot-spot could not be determined, but three-dimensional modelling indicated that it could be localised to a few tens of kilometres.

#### 4.2. MATURE OCEANIC LITHOSPHERE

Lizzeralde et al. (1995), and Heinson and Lilley (1993) determined the conductivities of mature oceanic lithosphere and asthenosphere in the northeastern Pacific Ocean and Tasman Sea respectively. Lizzeralde et al. used a seafloor cable to monitor electric potential differences between mainland USA and Hawaii, and determined MT transfer functions using magnetic field data from Hawaii. In analysis of the data, Lizzeralde et al. found evidence for an HCZ (0.05–0.1 S/m) between

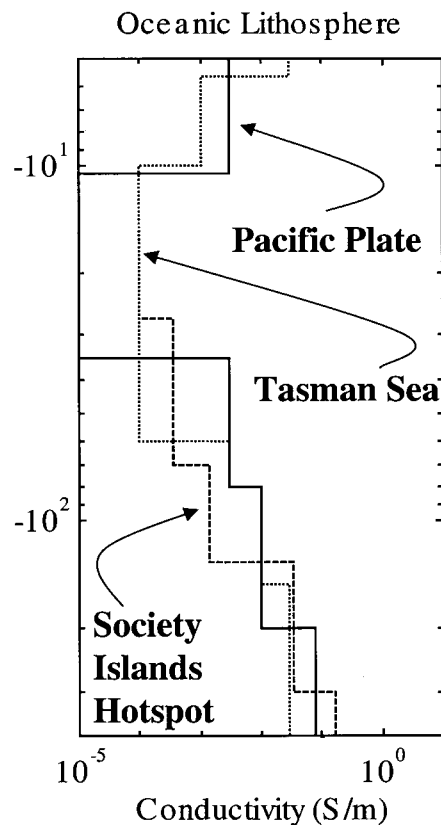


Figure 7. Ocean lithosphere conductivity structures for the northeast Pacific Ocean (solid line; Lizzeralde et al., 1995), Tasman Sea (dotted line; Heinson and Lilley, 1993) and above the Society Islands hot-spot (dashed-line; Nolasco et al., 1998).

150 and 400 km depth, as shown in Figure 7. Such conductivities are higher than would be expected from temperature-dependent olivine or lherzolite conduction. Lizzeralde et al. argue that either there is gravitationally stable melt (1–3%) in situ, or that hydrogen solubility and diffusivity in olivine can provide the necessary conductivity (Karato, 1990). The latter hypothesis requires that the olivine [100] axis be aligned over these depths, approximately parallel to the direction of the cable.

Heinson and Lilley (1993) used thin-sheet modelling to interpret MT data from the Tasman Sea. Distortion in the data was largely due to the coastlines and bathymetry, and the upper mantle was found to be mostly uniform in lateral conductivity. The one-dimensional structure below the Tasman Sea is shown in Figure 7. There is good agreement between the Tasman Sea model and the northeastern Pacific Ocean model, particularly at depths below 100 km. The conductivity of oceanic lithosphere is hard to determine from MT studies due to the very low values ( $<0.0001$  S/m). Some constraints are provided by low-frequency controlled source

EM (Flosadottir and Constable, 1996; Constable and Cox, 1996) which can place bounds to depths of 60 km.

In the case of the northeastern Pacific Ocean and Tasman Sea, the oceanic lithosphere is between 30 and 90 Ma old, and should have a rheological thickness of 60–80 km. Although there is an increase in conductivity beginning at these depths, the peak conductivity occurs below 150 km (see also Ferguson et al., 1990). There appears, therefore, to be a difference between the rheological and electrical properties of the asthenosphere. One possible explanation is that melt fraction increases with depth through the asthenosphere, reaching a maximum at 150 km. Alternatively, mobile hydrogen ions below depths of 150 km in the mantle may enhance conduction (Karato, 1990). If hydrogen ions are responsible for high conductivities over depths 150–300 km, then this part of the upper mantle will be anisotropic (Constable, 1993).

Everett and Constable (1998) detect conductivity anisotropy in the upper-mantle just below the Moho of almost an order of magnitude. Such anisotropy presumably results from conduction along the [1 0 0] axis of olivine that is orientated parallel to the direction of spreading. White et al. (1997) interpreted data from EMSLAB and the Tasman Sea, and showed there to be conductive structures which parallel the direction of spreading. More studies are needed to make progress in determining anisotropy as a function of depth through the oceanic lithosphere and asthenosphere.

#### 4.3. HOT-SPOTS

Nolasco et al. (1998) report on MT measurements around Tahiti, and determine a two-dimensional model of the Society Islands hot-spot. The conductivity profile beneath the hot-spot is shown in Figure 7. Contrary to expected high conductivities below the lithosphere, Nolasco et al. found lower conductivities, which they attribute to the melt extraction and subsequent dehydration of the mantle. Below 150 km, the model agrees well with the lithosphere models of Lizzeralde et al. and Heinson and Lilley. Another recent MT experiment on a hot-spot was carried out around the Hawaiian superswell (S.C. Constable, pers. comm., 1998), known as the SWELL experiment. A relatively uniform lithosphere conductivity of 0.005 S/m was observed, with evidence of higher conductivity beneath the islands.

#### 4.4. PASSIVE MARGINS

Passive margins should contain an electrical conductivity signature from episodes of continental rifting, subsequent seafloor spreading and in some cases fossil subduction. Oceanic lithosphere will grade into continental lithosphere, and asthenosphere will be deeper under the continental side. Ogawa et al. (1996) report on the SOAP (Southern Appalachian) experiment, which constitutes a land arid marine MT and GDS transect across the southeast Appalachian Mountains. Data from the marine experiment are being analysed at present. Land-based MT data

close to the coast indicate a resistive structure from 0.0001–0.001 S/m over the top 125 km, below which is a conductive region of 0.1 S/m. The interpretation of the inland section will be discussed later in this paper.

White and Heinson (1994) discuss a land-marine transect of magnetometers across the Proterozoic southern Australian coastline. From GDS and vertical gradient sounding (VGS) data, they interpreted a passive margin profile with an upper mantle of between 0.001 and 0.003 S/m to 400 km and <0.3 S/m below 400 km. No indication of either an electrical asthenosphere or a difference in lithosphere conductivity across the coastline was found.

## 5. EM Studies of Continental Lithosphere and Asthenosphere

Brown (1994) and Hjelt and Korja (1993) have given recent reviews of continental EM studies. As would be expected, there are many more continental than oceanic lithosphere-asthenosphere experiments. Magnetotellurics is the main EM method used, but long period GDS also provide constraints on mantle structures. Data density can be significantly higher on land, thus more detailed images of upper mantle conductivity have been determined. The picture that emerges is that continental lithosphere is much more heterogeneous than the oceanic lithosphere. Within continental Europe, for example, Hjelt and Korja (1993) show that electrical asthenosphere depths can vary from greater than 200 km to less than 40 km over distances of only a few hundred kilometres.

### 5.1. CONTINENTAL SHIELDS

A number of MT experiments have been performed above shield areas in the last ten years. In Canada, Schultz et al. (1993) imaged upper mantle conductivity using long-period MT records from Carty Lake, Ontario. The authors report jumps in the conductivity profile at depths near the major upper mantle seismic discontinuities (Lehmann discontinuity at 230 km depth, the transition zone depth of 400 km, and at 670 km), as shown in Figure 8. There is no evidence for an electrical asthenosphere because conductivities are less than 0.01 S/m over the top 200 km (similar to what might be expected from the 502 model of olivine conductivity). Lizzeralde et al. (1995) note that the conductivity structure beneath the shield is much less than for the oceanic lithosphere in northeastern Pacific Ocean, and beneath the Basin and Range Province in continental USA (Egbert and Booker, 1992).

Kellett et al. (1993), Kurtz et al. (1993), Maresehal et al. (1995) and Shaocheng et al. (1996) have reported some of the most exciting work above shields. Magnetotelluric data collected in the Superior Subprovince of the Canadian Shield show that the upper mantle is anisotropic in conductivity, but does not indicate an electrical asthenosphere (see Figure 8). The top of the anisotropic layer ranges from 45 km to 65 km, a change in depth that parallels the depth of the Moho determined from seismic data. The thickness of the anisotropic region is not well constrained, but should



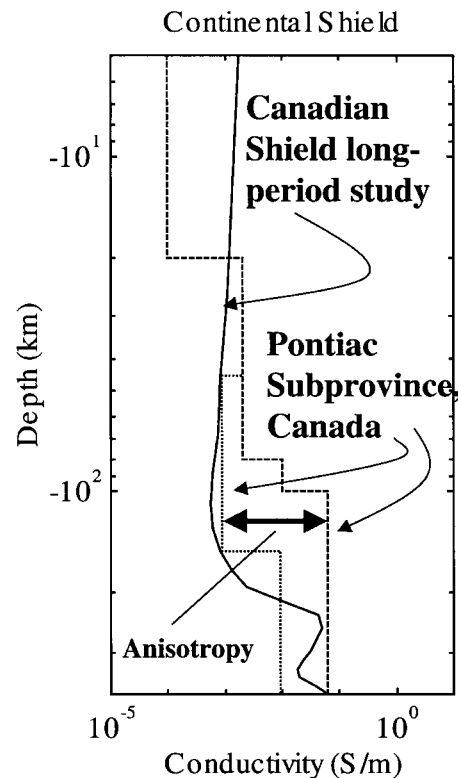


Figure 8. Continental shield conductivity structures beneath the Canadian Shield. The solid line shows the long-period MT inversion of Schultz et al. (1993), the dashed and dotted lines show inversions of data from one site on the Pontiac Subprovince (Mareschal et al., 1995). The difference between the dashed and dotted lines indicates the conductivity anisotropy in the upper mantle below 45 km depth.

be less than 150 km based on the long-period soundings of Schultz et al. (1993). There exists an obliquity between seismic and electrical anisotropy; Shaocheng et al. (1996) suggest that these are due to lattice-preferred and shape-preferred orientations of mantle minerals respectively. Mareschal et al. (1995) argue that the electrical conductivity anisotropy can be explained by conducting graphite films along fractures or grain boundaries, resulting from metasomatism of the mantle roots of major shear zones that transect the entire Superior Subprovince. From this evidence it appears that the upper mantle beneath the shield has remained in place since Archaean times. It is interesting to note that regions adjacent to the Superior Subprovince such as the Grenville Province show little to no anisotropy, due to late Proterozoic metamorphism which “resets” the upper mantle (Mareschal et al., 1995).

An electrical asthenosphere is also absent under most of the Fennoscandian Shield under Finland and Sweden (Hjelt and Korja, 1993; Korja, 1993; Korja and

Hjelt, 1993; Korja and Koivukoski, 1994), although there is some evidence of an electrical asthenosphere beneath southern Sweden. Moroz and Pospeev (1995) show that the conductivity beneath the Siberian Shield is about 0.02 S/m at a depth of 320 km, indicating a lack of an electrical asthenosphere.

## 5.2. CONTINENTAL AND ISLAND ARC SUBDUCTION ZONES

Over the last ten years, a large-scale MT and seismic experiment has been conducted across the Andes and Cordilleras in Chile (Schwarz et al., 1994; Schwarz and Krüger, 1998; Echternacht et al., 1997). The Central Andes are of global significance as a classic example of a Cordilleran orogeny, with subduction at the continental margin and dominantly compressional tectonics on land. Subduction is extremely active (compared to the EMSLAB experiment where subduction was virtually passive), driven by a relative plate velocity of 10 cm/yr. The main results from this experiment are that very high conductivities of 0.5–2 S/m are imaged at crust and sub-Moho depths of 70–180 km (Figure 9) directly beneath the Western Cordilleras, presumably melt diapirs of width 50 km, rising from subducted plate. Between the subduction zone and the Western Cordilleras, the upper mantle is modelled with conductivity 0.0001 S/m to a depth of 300 km, below which it is 0.05 S/m. Modelling to date has been primarily one- and two-dimensional, and with increasing data coverage it will be interesting to see a three-dimensional EM view of a rising diapir.

Pous et al. (1995a, b) report on a magnetotelluric profile through the central Pyrenees in Europe, which marks the boundary between the Iberian and European plates. The authors suggest that an HCZ observed in the mantle of conductivity 0.3 S/m is due to melting of subducted crustal material during the Pyrenean continental collision. Asthenosphere depths are estimated to be 80 km south of the Pyrenees and 115 km to the north. Unlike the Central Andes, there is no evidence of magmatism at the surface; the authors suggest that melt is trapped as lithosphere extension has not resulted in extensional faulting.

Jones and Gough (1995) and Majorowicz et al. (1993) summarise the results of over 400 MT soundings in the Canadian Cordillera a region of recent accretions of crustal terranes to North America. A thin-crust (32 km) under the Omineca Belt and an electrical asthenosphere at 40 km suggest that the lower crust is partially molten. Jones and Gough (1995) suggest that the thin-lithosphere could be due to extension.

Other continental subduction studies include those in Kamchatka, eastern Russia and Sakhalin Island by Semenov and Rodkin (1996), Moroz and Pospeev (1995) and Mishin (1996). An asthenospheric HCZ layer (1996) undergoes uplift towards the Pacific Ocean and (1997) rises towards the surface of Kamchatka, an area of recent volcanism and hydrothermal activity. Island arc and continent-continent subduction zones studies have continued in New Zealand (Chen et al., 1993; Ingham, 1996a, 1996b; Wannamaker et al., 1997) and Japan (e.g., Handa et al., 1992; Fujita

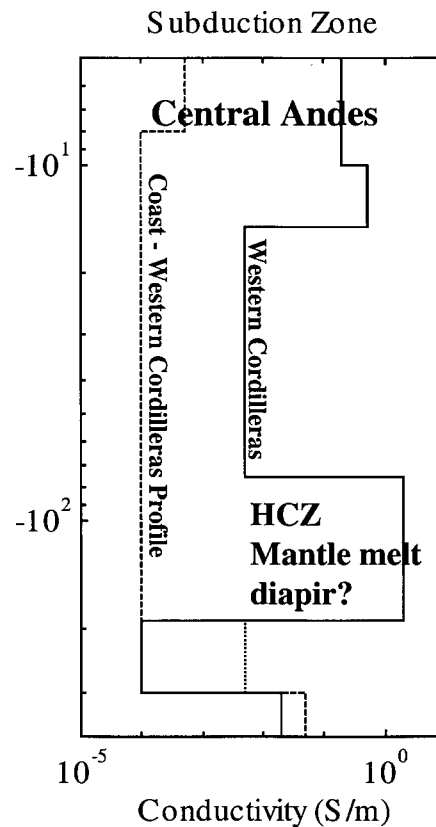


Figure 9. Conductivity profiles above the Central Andes subduction zone in Chile, adapted from Echemacht et al. (1997). The solid line shows the structure under the Western Cordillera; high conductivities are seen in the crust, and a rising melt diapir is imaged between about 75 and 180 km. The dashed line shows the conductivity between the Western Cordillera and the coastline.

et al., 1997; Fujinawa et al., 1997). Although most of this work has been directed to the delineation of crustal structure, some constraints on the lower subducting slab can be obtained.

### 5.3. CONTINENTAL LITHOSPHERE EXTENSION AND COMPRESSION ZONES

Park et al. (1995, 1996) report on a MT and seismic experiment across the southern Sierra Nevada in the western side of the USA. In this region, extension in the Basin and Range province produces lithospheric thinning. In the eastern side of the Sierras the authors find evidence for enhanced conductivities in the mantle to depths in excess of 100 km, which is attributed to partial melting. At the western side of the array, beneath the western foothills of the Sierras and the Great Valley sediments, a second conductive sub-Moho feature was identified. In this region the

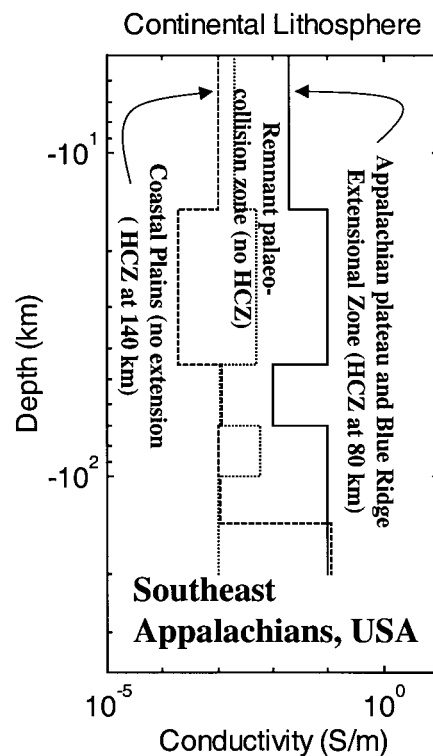


Figure 10. Examples of conductivity profiles beneath the southeastern Appalachians, USA, from the SOAP experiment (Ogawa et al., 1996). Three profiles are shown, 200 km apart, adapted from a full 2D inversion of data. The solid line shows conductivity beneath the Appalachian plateau arid Blue Ridge extensional region, with high conductivities in the lower crust (15–45 km depth), and a conductive upper mantle region below 80 km. The dashed line is for the coastal plains; no crustal conductor is imaged, but a conductive upper mantle begins at 140 km. In between these regions, the dotted line shows no upper mantle conductor, possibly representing the remnant structure of a palaeo-collision zone.

authors suggest that the high conductivity is due to graphitic metasediments and/or dehydration of metaserpentinite.

The SOAP experiment (Wannamaker et al., 1996; Ogawa et al., 1996) across the southeastern Appalachian Mountains identified two HCZs in the upper mantle (Figure 10). The Appalachians are an ancient fold belt, reactivated as a zone of extension. However, as for the shield studies (Maresehal et al., 1995) the crust and upper mantle retain a signature of part orogenic events. The electrical asthenosphere (0.1 S/m) is shallower under the Appalachian plateau (at 80 km depth) than in the coastal zone (140 km). Between the two regions, there is a 200 km wide resistive gap in the upper mantle, which the authors suggest is a remnant structure of the Alleghanian collision.

Variations in lithosphere thickness and asthenosphere depth have been extensively mapped across Europe; Hjelt and Korja (1993) provide an extensive review

of recent work. Across Europe, a variety of extensional and compressional regions exist (Babuska and Plomerova, 1992; Praus and Pecova, 1994; Cerv et al., 1997a). The Carpathian Mountain chain was formed from the collision between the Variscan European continent and the microplates in front of the African plate. The extensional Pannonian Basin lies to the south and west of the Carpathian Mountains. Adam (1997), Adam et al. (1993, 1996), Adam and Steiner (1993) and Posgay et al., (1995, 1996) have developed extensive data sets and models for the Pannonian Basin in Hungary. The authors found the electrical asthenosphere to be at an average depth of 50–70 km, but beneath the Bekes graben the electrical asthenosphere shallows to 40 km. To the north and east of the Pannonian Basin (Semenov et al., 1993; Lankis et al., 1995; Burakhovich et al., 1995; Cerv et al., 1997a) similar MT experiments have shown patterns of lithospheric thickening beneath fold belts and thinning with extension. Burakhovich et al., for example, detect partial melt at a depth of 40 km in an extensional basin in Ukraine, adjacent to a shield area with an electrical asthenosphere at a depth of > 150 km.

North and west of the Carpathians lie the tectonic units of the Variscan belt in Germany and northern Europe. Tezkan (1994) finds evidence for a highly conducting layer (0.01 S/m) in the upper mantle at 120 km depth beneath the Rhine-Graben, which is interpreted as an electrical asthenosphere (see also Cerv et al., 1997b). Similar deep structure was detected by Braitenberg et al. (1994) beneath the Friuli region of northeast Italy. The Alpine belt which separates this region shows a deeper upper mantle conductor at 200 km (Bahr, 1992).

Elsewhere, in India Singh et al. (1995) collected MT data near the southern boundary of the Indo-Gangetic basin. They found evidence for a very resistive upper mantle. In China, Qin-Guo-Qing et al. (1994) identified an asthenosphere at a depth of 100 km north of Tibet. Chen et al. (1996) are currently investigating Tibetan crustal structure. Wannamaker et al. (1996, 1997) discuss recent MT measurements in Antarctica above the Byrd Subglacial Basin, which is in a dormant state of rifting. Conductivities of the order of 0.0005 S/m to 100 km depth were identified.

## 6. Conclusions

Although there are few studies of oceanic lithosphere-asthenosphere, they indicate a relatively uniform conductivity structure, except at mid-ocean ridges and subduction zones. Directly beneath mid-ocean ridges there is some evidence for high conductivities (0.1 S/m) and a partially molten asthenosphere at depths of 50–100 km. Melt fractions appear to be very small or absent beneath older seafloor at the depths of the seismic LVZ, but an HCZ (0.1 S/m) is imaged below 150 km depth. This deeper zone may have enhanced conductivities due to volatiles and/or melt. If volatiles (in the form of mobile hydrogen ions) are responsible for the observed high conductivities, then an anisotropy should be found, aligned with

the plate motion. Oceanic lithosphere is found to be highly resistive everywhere ( $<0.0001$  S/m).

A partially molten asthenosphere appears to be absent beneath continental shields. One of the most important discoveries is that the upper mantle is anisotropic beneath the Canadian Shield over depths of 45–150 km. Although seismic anisotropy in the same area is explained in terms of mineral orientation, it is argued that electrical conductivity must be due to the presence of graphite, deposited during episodes of mantle shear-zone formation during the Archaean. These studies suggest that, despite rheological weaknesses at the Moho beneath the Canadian Shield, the upper mantle has remained attached and part of the shield structure over the last 2 billion years. Similar studies of anisotropy in other shield areas of the world will be of great interest.

Our understanding of subduction zones beneath continents and island arcs continues to improve with fresh studies. Since the EMSLAB experiment and other studies of the Juan de Fuca Plate, EM methods have provided excellent constraints on the processes of subduction, de-watering and melting. The exciting work above the active subduction zone in the Central Andes clearly shows high conductivity zones (0.5–2 S/m) in the upper mantle with lateral and vertical dimensions of 50 and 100 km respectively, probably representative of melt diapirs rising from the subducted plate.

Electromagnetic studies in extensional continental basins show a thinning of the lithosphere and an asthenospheric partial melt zone at depths below 40–60 km. In various regions across the world (e.g., Pannonian Basin, central Europe; Basin and Range Province, USA) there appears to be good agreement between models of conductivity. In contrast, regions of compression are more resistive and have a weakly defined asthenosphere at depths of  $>140$  km. Extensive studies in Europe, Canada and USA show that the lithosphere-asthenosphere structure is complex in continental regions. Asthenosphere depths can range from 70 to 200 km in a little over 100 km laterally, implying either significant changes in upper mantle composition (e.g., palaeo-subduction zones beneath the Pyrennees) or major changes in geothermal gradients which are stable over long time-scales.

### Acknowledgements

I am very grateful to Dr Dumitru Stanica and the organising committee of the 14th EM Workshop in Sinaia, Romania for the invitation to present this review. Many colleagues promptly provided reprints and pre-prints that helped considerably, particularly in the field of mineral physics. Two referees provided many useful and constructive comments that have improved the quality of this manuscript. Finally, I would like to thank the Australian Research Council and Flinders University for funding to attend the workshop and present this work.

## References

- Adam, A.: 1997, 'Magnetotelluric phase anisotropy above extensional structures of the Neogene Pannonian Basin', *J. Geomag. Geoelect.* **49**, 1549–1557.
- Adam, A. and Steiner, T.: 1993, 'Effect of deep reaching tectonics on conductivity structure in the Pannonian basin, can magnetotelluric data constrain tectonic interpretations?', *Phys. Earth Planet. Int.* **81**, 1–8.
- Adam, A., Szarka, L., and Steiner, T.: 1993, Magnetotelluric approximations for the asthenospheric depth beneath the Bekes Graben, Hungary', *J. Geomag. Geoelect.* **45**, 761–773.
- Adam, A., Szarka, L., Pracser, E. and Varga, G.: 1996, 'Mantle plumes of EM distortions in the Pannonian Basin? (Inversion of the deep magnetotelluric (MT) soundings along the Pannonian Geotraverse)', *Geophysical Transactions – Eotvos Lorand Geophysical Institute of Hungary* **40**, 45–78.
- Babuska, V. and Plomerova, J.: 1992, 'The lithosphere in central Europe – seismological and petrological aspects', *Tectonophysics* **207**, 141–163.
- Bahr, K.: 1992, 'The electrical asthenosphere under the Alps', paper presented at *The Hutton Symposium, European Geophysical Society*, Edinburgh.
- Braitenberg, C., Capuano, P., Gasparini, P. and Zadro, M.: 1994, 'Interpretation of long period magnetotelluric soundings in Friuli (northeast Italy) and the electrical characteristics of the lithosphere', *Geophys. J. Int.* **117**, 196–204.
- Brown, C.: 1994, 'Tectonic interpretation of regional conductivity anomalies', *Surveys in Geophysics* **15**, 123–157.
- Burakhovich, T.K., Kulik, S.N. and Logvinov, I.M.: 1995, 'Goelectrical model of the Earth's crust and upper mantle in the Cis Dobruja Trough and North Dobruja', *Geophysical Journal* **15**, 613–623.
- Cathies, L.M., 1975, *The Viscosity of the Earth's Mantle*, Princeton University Press, N.J.
- Cerv, V., Kovackova, S., Pek, J., Pecova, J. and Praus, O.: 1997a, 'Model of electrical conductivity distribution across central Europe', *J. Geomag. Geoelect.* **49**, 1585–1600.
- Cerv, V., Pek, J., and Praus, O.: 1997b, 'The present state of art of long period magnetotellurics in the western part of the Bohemian Massif', *J. Geomag. Geoelect.* **49**, 1559–1583.
- Chen, J., Dosso, H.W., and Ingham, M.: 1993, 'Electromagnetic induction in the New Zealand South Island', *Phys. Earth Planet. Int.* **81**, 253–260.
- Chen, L., Booker, J.R., Jones, A.G., Wu, N., Unsworth, M., Wei, W., and Tan, H.: 1996, 'Electrically conductive crust in southern Tibet from INDEPTH magnetotelluric surveying', *Science* **274**, 1694–1696.
- Constable, S.C.: 1993, 'Conduction by mantle hydrogen', *Nature* **362**, 704.
- Constable, S.C. and Duba, A.: 1990, 'Electrical conductivity of olivine, a dunite, and the mantle', *J. Geophys. Res.* **95**, 6967–6978.
- Constable, S.C., Shankland, T.J., and Duba, A.: 1992, 'The electrical conductivity of an isotropic olivine mantle', *J. Geophys. Res.* **97**, 3397–3404.
- Constable, S.C. and Cox, C.S.: 1996, 'Marine controlled source electromagnetic sounding 2. The PEGASUS experiment', *J. Geophys. Res.* **101**, 5519–5530.
- Constable, S.C., Heinson, G.S., Anderson, G. and White, A.: 1997, 'Seafloor electromagnetic measurements above Axial Seamount', *J. Geomag. Geoelect.* **49**, 1327–1342.
- Duba, A. and Constable, S.C.: 1993, 'The electrical conductivity of lherzolite', *J. Geophys. Res.* **98**, 11,885–11,899.
- Echternacht, F., Tauber, S., Eisel, M., Brasse, H., Schwarz, G., and Haak, V.: 1997, 'Electromagnetic study of the active continental margin in northern Chile', *Phys. Earth Planet. Int.* **102**, 69–87.
- Echternacht, F., Tauber, S., Eisel, M., Brasse, H., Schwarz, G., and Haak, V.: 1997, 'Electromagnetic study of the active continental margin in northern Chile', *Phys. Earth Planet. Int.* **102**, 69–87.

- Egbert, G.D. and Booker, J.R.:1992, 'Very long period magnetotellurics at Tucson observatory: Implications for mantle conductivity', *J. Geophys. Res.* **97**, 15,099–15,112.
- Evans, R.L., Tarits, P., Chave, A.D., Heinson, G.S., White, A., Filloux, J.H., Toh, H., Seama, N., Utada, H., Booker, J.R., and Unsworth, M.J.: 1999, 'Asymmetric Mantle Electrical Structure Beneath the East Pacific Rise at 17°', *Science*, in press.
- Everrett, M. and Constable, S.C.: 1999, 'Electric dipole fields over an anisotropic seafloor', *Geophys. J. Int.* **136**, 41–56.
- Faul, U.H.: 1997, 'Permeability of partially molten upper mantle rocks from experiments and percolation theory', *J. Geophys. Res.* **102**, 10,299–10,311.
- Faul, U.H., Toomey, D.R., and Waff, H.S.: 1994, 'Intergranular basaltic melt is distributed in thin, elongated inclusions', *Geophys. Res. Lett.* **21**, 29–32.
- Ferguson, I.J., Lilley, F.E.M. and Filloux, J.H.:1990, 'Geomagnetic induction in the Tasman Sea and the electrical conductivity structure beneath the Tasman Seafloor', *Geophys. J. Int.* **102**, 299–312.
- Filloux, J.H.: 1987, 'Instrumentation and experimental methods for oceanic studies', in J.A. Jacobs (ed.), *New Volumes in Geomagnetism*, Vol. 1, Academic Press, New York, pp. 143–246.
- Flosadottir, A.H. and Constable, S.C.: 1996, 'Marine controlled source electromagnetic sounding 1. Modeling and experimental design', *J. Geophys. Res.* **101**, 5507–5517.
- Forsyth, D.W. and Chave, A.D.: 1994, 'Experiment investigates magma in the mantle beneath mid Ocean ridges', *EOS* **75**, 537–540.
- Fujinawa, Y., Kawakami, N., Asch, T.H., Uyeshima, M. and Honkura, Y.: 1997, 'Studies of georesistivity structure in the central part of northeastern Japan arc', *J. Geomag. Geoelect.* **49**, 1601–1617.
- Fujita, K., Ogawa, Y., Yamaguchi, S. and Yaskawa, K.: 1997, 'Magnetotelluric imaging of the SW Japan forearc – a lost palaeoland revealed?', *Phys. Earth Planet. Int.* **102**, 231–238.
- Ghio, M.S. and Sack, R.O.: 1995, 'Chemical mass transfer in magmatic processes. IV. A revised and internally consistent thermodynamic model of the interpolation and extrapolation of liquid solid equilibria in magmatic systems at elevated temperatures and pressures', *Contributions to Mineralogy and Petrology* **119**, 197–212.
- Hagar, B.H. and O'Connell, R.: 1979, 'Kinematic models of large-scale flow in the Earth's mantle', *J. Geophys. Res.* **84**, 1031–1048.
- Handa, S., Tanaka, Y., and Suzuki, A.: 1992, 'The electrical high conductivity layer beneath the northern Okinawa Trough, inferred from geomagnetic depth sounding in northern and central Kyushu, Japan', *J. Geomag. Geoelect.* **44**, 505–520.
- Heinson, G.S. and Lilley, F.E.M.: 1993, 'An application of thin sheet electromagnetic modelling to the Tasman Sea', *Phys. Earth Planet. Int.* **81**, 231–251.
- Heinson, G.S., White, A., Law, L.K., Hamano, Y., Utada, H., Yukatake, T., Segawa, H., and Toh, H.: 1993, 'EMRIDGE: the electromagnetic investigation of the Juan de Fuca Ridge', *Mar. Geophys. Res.* **15**, 77–100.
- Heinson, G., Constable, S.C., and White, A.: 1996, 'Seafloor magnetotelluric sounding above Axial Seamount', *Geophys. Res. Lett.* **23**, 2275–2278.
- Hirsch, L.M., Shankland, T.J., and Duba, A.: 1993, 'Electrical conduction and mobility in Fe-bearing olivine', *Geophys. J. Int.* **114**, 36–44.
- Hirth, G. and Kohlstedt, D.L.: 1996, 'Water in the oceanic upper mantle: Implications for rheology, melt extraction and the evolution of the lithosphere', *Earth Planet. Sci. Lett.* **144**, 93–108.
- Hjelt, S.E. and Korja, T.: 1993, 'Lithospheric and upper mantle structures, results of electromagnetic soundings in Europe', *Phys. Earth Planet. Int.* **79** 137–177.
- Ingham, M.: 1996a, 'Magnetotelluric sounding across the Southern Alps orogeny, South Island of New Zealand: Data presentation and preliminary interpretation', *Phys. Earth Planet. Int.* **94**, 291–306.
- Ingham, M.: 1996b, 'Magnetotelluric soundings across the South Island of New Zealand: Electrical structure associated with the orogen of the Southern Alps', *Geophys. J. Int.* **124**, 134–148.



- Jegen, M. and Edwards, R.N.: 1998, 'The electrical properties of a two-dimensional conductive zone under the Juan de Fuca Ridge', *Geophys. Res. Lett.* **25**, 3647–3650.
- Jones, A.G. and Gough, D.I.: 1995, 'Electromagnetic images of crustal structures in southern and central Canadian Cordillera', *Canadian Journal of Earth Sciences* **32**, 1541–1563.
- Karato, S.: 1990, 'The role of hydrogen in the electrical conductivity of the upper mantle', *Nature* **347**, 272–273.
- Kellett, R.L., Mareschal, M. and Kurtz, R.D.: 1992, 'A model of lower crustal electrical anisotropy for the Pontiac Subprovince of the Canadian Shield', *Geophys. J. Int.* **111**, 141–150.
- Korja, T. and Hjelt, S.E.: 1993, 'Electromagnetic studies in the Fennoscandian Shield – electrical conductivity of Precambrian crust', *Phys. Earth Planet. Int.* **81**, 107–138.
- Korja, T., and Koivukoski, K.: 1994, 'Crustal conductors along the SVEKA profile in the Fennoscandian (Baltic) Shield, Finland', *Geophys. J. Int.* **116**, 173–197.
- Korja, T.: 1993, 'Electrical conductivity distribution of the lithosphere in the central Fennoscandian Shield', *Precambrian Res.*
- Kurtz, R.D., Craven, J.A., Niblett, E.R., and Stevens, R.: 1993, 'The conductivity of the crust and mantle beneath the Kapuskasing Uplift: Electrical anisotropy in the upper mantle', *Geophys. J. Int.* **113**, 483–498.
- Lankis, L.K., Kulik, S.N., and Lysenko, E.S.: 1995, 'Results of numerical modelling of the deep geoelectrical section of the seismically active areas of the Eastern Carpathians and adjoining regions' *Geophys. J.* **15**, 437–447.
- Lay, T. and Wallace, T.C.: 1995, *Modern Global Seismology*, Academic Press, 521 pp.
- Lizarralde, D., Chave, A., Hirth, G., and Schultz, A.: 1995, 'Northeastern Pacific mantle conductivity profile from long period magnetotelluric sounding using Hawaii to California submarine cable data', *J. Geophys. Res.* **100**, 17,837–17,854.
- Majorowicz, J.A., Gough, D.I., and Lewis, T.J.: 1993, 'Electrical conductivity and temperature in the Canadian Cordilleran crust', *Earth and Planet. Sci. Lett.* **115**, 57–64.
- Mareschal, M., Kellett, R.L., Kurtz, R.D., Ludden, J.N., Ji, S., and Bailey, R.C.: 1995, 'Archaean cratonic roots, mantle shear zones and deep electrical anisotropy', *Nature* **375**, 134–137.
- McKenzie, D.P.: 1989, 'Some remarks on the movement of small melt fractions in the mantle', *Earth Planet. Sci. Lett.* **74**, 81–91.
- Mishin, V.V.: 1996, 'Deep structure and the types of crust of South Kamchatka', *Geology of The Pacific Ocean* **13**, 145–159.
- Molnar, P.: 1998, 'Continental tectonics in the aftermath of plate tectonics', *Nature* **355**, 131–137.
- Moroz, Yu.F., and Pospeev, A.V.: 1995, 'Deep electrical conductivity of east Siberia and the far east of Russia', *Tectonophysics* **245**, 85–92.
- Nolasco, R., Tarits, P., Filloux, J.H. and Chave, A.D.: 1998, 'Magnetotelluric imaging of the Society Islands Hot Spot', *J. Geophys. Res.* **103**, 30287.
- Ogawa, Y., Jones, A.G., Unsworth, M.J., Booker, J.R., Xinyou Lu, Craven, J., Roberts, B., Parmelee, J., and Farquharson, C.: 1996, 'Deep electrical conductivity structures of the Appalachian Orogen in the southeastern US', *Geophys. Res. Lett.* **23**, 1597–1600.
- Paishin, N.A.: 1996, 'Oceanic electromagnetic studies: A review', *Surveys in Geophysics* **17**, 455–491.
- Park, S.K., Clayton, R.W., Ducea, M.N., Wernicke, B., Jones, C.H., and Ruppert, S.D.: 1995, 'Project combines seismic and magnetotelluric surveying to address the Sierran root question', *EOS* **76**, 297–298.
- Park, S.K., Hirasuna, B., Jiracek, G.R., and Kirin, C.: 1996, 'Magnetotelluric evidence of lithospheric mantle thinning beneath the southern Sierra Nevada', *J. Geophys. Res.* **101**, 16241–16255.
- Parkinson, W.D.: 1983, *Introduction to Geomagnetism*, Scottish Academic Press., 433 pp.
- Parsons, B. and Sclater, J.G.: 1977, 'An analysis of the variation of ocean floor bathymetry and heat flow with age', *J. Geophys. Res.* **82**, 803–827.

- Posgay, K., Albu, I., Adam, A., Berczi, I., Hegedus, E., Janvarine, K.I., Kovacsvolgyi, S., Lenkey, L., Nagy, Z., Papa, A., Redlerne., T.M., Sipos, J., Stegena, L., Szafian, P., Szalay, A., Timar, Z., Takacs, E., and Varga, G.: 1995, 'Deep reflection survey of the pre Tertiary basement', *Magyar Geofizika* **36**, 27–36.
- Posgay, K., Takacs, E., Szalay, I., Bodoky, T., Hegedus, E., Kantor, J.I., Timar, Z., Varga, G., Berczi, I., Szalay, A., Nagy, Z., Papa, A., Hajnal, Z., Reilkoff, B., Mueller, S., Ansoerge, J., De Iaco, R., and Asudeh, I.: 1996, 'International deep reflection survey along the Hungarian Geotraverse', *Geophysical Transactions, Eotvos Lorand Geophysical Institute of Hungary* **40**, 1–44.
- Pous, J., Ledo, J., Marcuello, A., Daignieres, M.: 1995, 'Electrical resistivity model of the crust and upper mantle from a magnetotelluric survey through the central Pyrenees', *Geophys. J. Int.* **121**, 750–762.
- Pous, J., Munoz, J.A., Ledo, J. J., and Liesa, M.: 1995, 'Partial melting of subducted continental lower crust in the Pyrenees', *Journal Geological Society (London)*, **152**, 217–220.
- Praus, O. and Pecova, J.: 1994, 'Deep electrical structure under Central Europe', *Studia Geophysica Et Geodaetica* **38**, 57–70.
- Qin Guo Qing, Chen Jiu Hui, Liu Da Ji an, Gu Qun, Xiong Yang Wu, and Li Hai Xiao: 1994, 'The characteristics of the electrical structure of the crust and upper mantle in the region of the Kunlun and the Karakorum Mountains', *Acta Geophysica Sinica* **37**, 193–199.
- Roberts, J.J. and Tyburczy, J.A.: 1991, 'Frequency dependent electrical properties of polycrystalline olivine compacts', *J. Geophys. Res.* **96**, 16205–16222.
- Roberts, J.J. and Tyburczy, J.A.:1993, 'The frequency dependent electrical properties of dunite as a function of temperature and oxygen fugacity', *Phys. Chem. Miner.* **19**, 545–561.
- Roberts, J.J. and Tyburczy, J.A.:1994, 'Frequency-dependent electrical properties of minerals and partial melts', *Surv. in Geophys.* **15**, 239–262.
- Roberts, J.J. and Tyburczy, J.A.: 1999, 'Partial-melt electrical conductivity: influence of melt composition', *J Geophys. Res.* **104**, 7055–7065.
- Ribe, N.: 1989, 'Seismic anisotropy and mantle flow', *J. Geophys. Res.* **94**, 4213–4223.
- Ringwood, A.E.: 1975, 'Composition and Petrology of die Earth's Mantle', McGraw Hill, New York.
- Schultz, A., Kurtz, R.D., Chave, A.D., and Jones, A.G.:1993, 'Conductivity discontinuities in the upper mantle beneath a stable craton', *Geophys. Res. Lett.* **20**, 2941–2944.
- Schwarz, G. and Kruger, D.: 1997, 'Resistivity cross section through the Southern Central Andean Crust as inferred from 2D modelling of magnetotelluric and geomagnetic deep sounding measurements', *J. Geophys. Res.* **102**, 11,957–11,978.
- Schwarz, G., Chong, G., Kruger, D., Martinez, M., Massow, W., Rath, V., and Viramonte, J.: 1994, 'Crustal high conductivity zones in the southern Central Andes', in K. Reutter, E. Scheuber, P. Wigger (eds.), *Tectonics of die Southern Central Andes*, Springer, Berlin.
- Semenov, V.Yu., Ernst, T., Jozwiak, W., and Pawliszyn, J.: 1993, 'The crust and mantle electrical conductivity estimation using Polish observatory data', *Acta Geophysica Polonica* **41**, 375–383.
- Semenov, V.Y., and Rodkin, M.: 1996, 'Conductivity structure of the upper mantle in an active subduction zone', *Journal of Geodynamics* **21**, 355–364.
- Shankland, T.J. and Waff, H.S.:1977, 'Partial melting and electrical conductivity anomalies in the upper mantle', *J. Geophys. Res.* **82**, 5,409–5,417.
- Shaocheng Ji, Rondenay, S., Mareschal, M., and Senechal, G.: 1996, 'Obliquity between seismic and electrical anisotropies as a potential indicator of movement sense for ductile shear zones in the upper mantle', *Geology* **24**, 1033–1036.
- Simpson, F.: 1999, 'Stress and seismicity in the lower continental crust: A challenge to simple ductility and implications for electrical conductivity mechanisms', *Surv. Geophys.*, in press.
- Singh, R.P., Kant, Y. and Vanyan, L.: 1995, 'Deep electrical conductivity structure beneath the southern part of the Indo Gangetic plains', *Phys. Earth Planet. Int.* **88**, 273–283.

- Sinha, M.C., Navin, D.A., MacGregor, L.M., Constable, S.C., Peirce, C., White, A., Heinson, G. and Inglis, M.A.: 1997, 'Evidence for accumulated melt beneath the slow spreading Mid Atlantic Ridge', *Phil. Trans. R. Soc. Lond.* **355**, 233–253.
- Su, W.J., Woodward, R.L. and Dziewonski, A.M.: 1994, 'Degree 12 model of shear velocity heterogeneity in the mantle', *J. Geophys. Res.* **99**, 6945–6980.
- Tanimoto, T. and Anderson, D.L.: 1984, 'Mapping convection in the mantle', *Geophys. Res. Lett.* **11**, 287–290.
- Tarits, P.: 1994, 'Electromagnetic studies of global geodynamic processes', *Surveys in Geophysics* **15**, 209–239.
- Tarits, P.: 1986, 'Conductivity and fluids in the oceanic upper mantle', *Phys. Earth Planet. Int.* **42**, 215–226.
- Tezkan, B.: 1994, 'On the detectability of a highly conductive layer in the upper mantle beneath the Black Forest crystalline using magnetotelluric methods', *Geophys. J. Int.* **118**, 185–200.
- Tozer, D.C.: 1979, 'The interpretation of upper mantle electrical conductivities', *Tectonophysics* **56**, 147–163.
- van der Hilst, R.D., Kennett, B.L.N. and Shibutani, T.: 1997, 'Upper mantle structure beneath Australia from portable array deployments', *AGU Geodynamics Series* **26**, 39–58.
- Wannamaker, P.E. and the EMSLAB group: 1989, 'Magnetotelluric observations across the Juan de Fuca subduction system in the EMSLAB project', *J. Geophys. Res.* **94**, 14,111–14,125.
- Wannamaker, P.E., Chave, A.D., Booker, J.R., Jones, A.G., Filloux, J.H., Ogawa, Y., Unsworth, M., Tarits, P., and Evans, R.: 1996, 'Magnetotelluric experiment probes deep physical state of southeastern US', *EOS* **77**, 329, 332–333.
- Wannamaker, P.E., Jiracek, G.R., Stodt, J.A., Caidwell, G., and McKnight, D.: 1997, 'Magnetotelluric investigation of the continent–continent plate boundary on the South Island of New Zealand: Observed data and preliminary 2D forward modeling', Presented at *Geophysical Investigation of a Modern Continent–Continent Collisional Orogen: The Southern Alps, New Zealand*, Principal Investigator Workshop, Wellington, February 1997.
- Wannamaker, P.E., Stodt, J.A., Olsen, S.L.: 1996, 'Dormant state of rifting below the Byrd Subglacial Basin, West Antarctica, implied by magnetotelluric (MT) profiling', *Geophys. Res. Lett.* **23**, 2983–2986.
- Watts, A.B., Bodine, J.H., and Steckler, M.S.: 1980, 'Observations of flexure and the state of stress in the oceanic lithosphere', *J. Geophys. Res.* **85**, 6369–6376.
- White, A. and Heinson, G.: 1984, 'Two dimensional electrical conductivity structure across the southern coastline of Australia', *J. Geomag. Geoelect.* **46**, 1067–1081.
- White, S.N., Chave, A.D. and Filloux, J.H.: 1997, 'A look at galvanic distortion in the Tasman Sea and the Juan de Fuca Plate', *J. Geomag. Geoelect.* **49**, 1373–1386.
- Xu, Y., Poe, B.T., Shankland, T.J. and Rubie, D.C.: 1998, 'Electrical conductivity of olivine, Wadsleyite, and Ringwoodite under upper-mantle conditions', *Science* **280**, 1415–1418.
- Zhang, Y. S. and Lay, T.: 1996, 'Global surface-wave phase velocity variations', *J. Geophys. Res.* **101**, 8415–8436.

